Long-Term Performance of a Multiplanar Positron Emission Tomograph

Kimberlee J. Kearfott

Department of Electrical and Computer Engineering Arizona State University, Tempe, Arizona

A protocol for the daily quality assurance (QA) of a multiplanar positron emission tomographic (PET) system was developed. This was implemented on a daily basis for the PC 4600 Neuro-PET, a multiplanar PET system designed for quantitative brain imaging. Sensitivity data collected as part of the protocol are presented for a 22-mo time period. These data show the need to periodically monitor instrument performance if meaningful quantitation is to be achieved. The methods presented have direct application to any quantitative multiplanar emission tomographic imaging program.

J Nucl Med 30: 1378–1385, 1989

One of the major advantages of positron emission tomography (PET) is its ability to provide regional quantitative information about in vivo physiology. However, quantitative metabolic imaging using PET requires accurate knowledge of the sensitivity of the PET camera. This sensitivity may vary gradually with time, or may change abruptly with sudden changes in technique or problems with instrumentation. A systematic monitoring of instrument sensitivity not only provides accurate and precise calibration information, but may also serve as a means of providing quality assurance (QA) for imaging procedures. Daily QA provides information about areas of the machine requiring tuning or servicing and may signal upcoming unacceptable degradations in instrument performance.

Any routine QA procedure should: (a) be easy to perform and repeatable, (b) require a minimum of time and operator interaction to complete, (c) test all relevant aspects of machine performance, (d) be sensitive to subtle and not-so-subtle variations in performance, (e) result in data in a form which is easy and quick to interpret, and (f) provide diagnostic information about problems which have developed.

This paper presents a plan implemented for the QA of The Cyclotron Corporation Model PC 4600 Neuro-PET, a five-ring neurologic PET system having 96 bismuth germanate (BGO) crystals per ring (*1*). It will include a discussion of the daily QA program, daily fluctuations in sensitivity, and the use of special statistical techniques such as multiple analysis of variance. Performance data obtained over a 22-mo period will be presented and analyzed. Calibration experiments utilizing a long, uniform phantom and a shorter, sectored linearity phantom will also be discussed. Use of a high count rate phantom and a hot spot imaging phantom for QA will also be mentioned. The general approach presented has broad application to other quantitative imaging devices. Several small enhancements to day-to-day operations and techniques which result in decreased variance in measurements of tissue radioactivity for PET will be discussed.

Received Nov. 28, 1988; revision accepted Apr. 21, 1989.

For reprints contact: Kimberlee J. Kearfott, School of Mechanical Engineering, Georgia Institute of Technology, Atlanta, GA 30332-0405.

METHODS

Empty Port Scans

The computer automatically tuned the detector energy thresholds each morning using a retractable, orbiting $^{68}Ge/^{68}Ga$ transmission rod source. The tuning was accomplished by varying the photomultiplier tube (PMT) amplifier gains to achieve a maximum count rate for a fixed window of ~300 to 700 keV (*1*). The resulting window was thus presumably centered on the photopeak. Because of the direct effect of energy window centering on count rate and the dependence of PMT gain on environmental factors such as temperature, daily tuning was of particular importance for instrument stability. In addition, the size of the window matched the photopeak size, making window positioning a particularly critical determinant of system sensitivity.

After tuning, 15-min empty port scans (EPS) were collected for wobbled and nonwobbled conditions. The total singles and coincidence counts for each detector were recorded. A total of ~18 to 30 million coincidence counts per plane were

collected for these EPS. The EPS included a correction for deadtime which was based upon observed count rates and equivalent deadtime per event. Whenever the rod source was utilized, such as for collection of the EPS, randoms were eliminated using an on-the-fly rod source masking technique followed by a singles counting based randoms correction method (*1*). Approximately 22 mo of this type of data were available for analysis of PET instrument drifts.

Daily PET QA

As an additional calibration and QA procedure following the collection of the EPS, the technician centered a 17.8-cm diameter, 30.5-cm-long uniform water-filled phantom using crossed lasers in the port. Alignment of the phantom was checked at several axial positions. The phantom had lines permanently etched in all three directions on its outer sides which marked both the transverse and axial centers and thus assisted in positioning in three dimensions. A 15-min wobbled transmission scan (TS) was obtained that contained ~6 to 10 million coincidence counts per plane. With the exception of rapid dynamic scans, the PET camera was used primarily in wobbled mode for most patient studies, hence nonwobbled scans were not typically obtained beyond the EPS.

Activity was eluted from a $^{68}Ge/^{68}Ga$ generator, which had a breakthrough of less than 3.2×10^{-6}. The long uniform phantom was filled with a known amount of isotope, typically 5.2 kBq cm^{-3} (0.14 μCi cm^{-3}) ^{68}Ga, as determined using a dose calibrator (Squibb Model CRC17 dose calibrator, Squibb Corporation, Princeton, NJ). Food coloring was added to the solution to ensure uniform mixing and to help in detecting spillage. The phantom was shaken for several minutes prior to use. An identical phantom filled with ^{68}Ge or another long-lived positron-emitting isotope would have simplified the daily procedure. However, such a phantom would have posed a problem of uniform phantom construction, not been ammenable to transmission scanning, and introduced complications with storage and shielding when not in use.

A wobbled emission scan (ES) was obtained, typically using a 10 to 40 min data collection. A total of 2 to 6 million coincidence counts per plane and a random-to-true ratio of <2% resulted. Reconstructions were made of the TS and ES to check for image artifacts. Detector inhomogeneity (relative sensitivity) correction factors were obtained from the raw projections of the EPS. Experimentally determined attenuation correction factors, based upon the ES and TS, were sometimes used for image reconstruction purposes. These images could reveal problems of instrument changes between the EPS and TS, or difficulties with the orbiting rod source. For long term data analysis purposes, however, analytic corrections were employed for attenuation to eliminate the statistical variations which would have been introduced by the TS. Randoms corrections based upon measured singles rates and deadtime corrections based upon observed count rate and equivalent deadtime per coincidence events were performed on the data at reconstruction time (*1*).

Upon completion of the ES, images of the daily PET QA phantom were reconstructed and visually examined for artifacts. Three samples were pipetted from the phantom, weighed and counted in the well counter (Bicron Model 2MW2/2 monoline well, Bicron, Newbury, OH; modified Picker Spectroscaler 4R assembly, Picker International, OH). The sensitivities for each plane and the well counter relative to the dose calibrator were then calculated based upon the total emission counts for each plane. Sensitivity data were obtained for the PC 4600 Neuro-PET in this manner on an almost daily basis for 3 mo during the installation of the machine and for more than 6 mo during its full clinical utilization.

The well counter was checked on a near-daily basis for drift using 33 kBq (0.9 μCi) and 1550 kBq (4.2 μCi) sodium-22 rod sources. Calibration of the dose calibrator was monitored on a monthly basis using standard cobalt-57, cesium-137, and cobalt-60 sources.

Phantom Positioning Accuracy

Axial couch position was provided for the patient couch using special digital encoders read by the PET camera/computer interface. The axial locations of each ring relative to the laser system were determined by moving a thin source of activity, a paper towel saturated with activity and sandwiched between two lucite blocks, axially through the port. Those positions at which maximum count rates were obtained, as indicated by a real time channel monitor, were noted. A captive rail was added to the couch to prevent its lateral motion during insertion into the scanner port and to ensure repeatable repositioning. To aid in vertical repositioning, a linear potentiometer was anchored to the base and on the movable section of the couch so that a digital position readout of the height of the couch above the floor was provided.

The effects of position on system sensitivity were examined by scanning the uniform phantom used for daily QA both centered and 1 cm above its centered position. Phantom position was expected to be accurate to within <2 mm in all directions because of the usage of crossed lasers (*2*). Similarly, typical variations in patient positioning were expected to be <1 cm because of the use of a specially designed patient headholder which restricts motion in all three directions (*3*).

Weekly and Monthly PET QA

Additional weekly and monthly phantom experiments were performed to supplement the daily uniform phantom tests. These included linearity, count rate capability, and overall imaging quality tests.

Linearity. On a semi-monthly basis, a previously published procedure was used to verify the linearity of system performance (*4*). A 20-cm diameter, 4.9-cm-long "pie" phantom containing five 270.5 cm^3 compartments covering 72° each was filled with a variety of different radioactivity concentrations. Use of a longer phantom would have allowed a simultaneous linearity test on all planes, with a considerable time savings. Activity concentrations of 3.7 to 259 kBq cm^{-3} (0.1–7 μCi cm^{-3}) of ^{68}Ga, as determined using a dose calibrator, were employed. The phantom was centered on a pre-selected ring and scanned for two or more half lives to verify linearity of the instrument. Aliquots of radioactivity were taken from each compartment following the scanning procedure and counted in the well counter.

Reconstructions of the linearity phantom were performed in a manner identical to patient studies, including experimental attenuation, random subtraction, detector inhomogeneity and deadtime corrections (*1*). Three 1–8 cm^2 regions of interest (ROIs) were selected per compartment in the final images. These were placed in an approximate equilateral triangle centered within each compartment so that the edges of the compartments and phantom were avoided. Specially written

software read these ROIs from a data file and fit a straight line to the resulting counts per pixel as a function of the activity concentration computed for each compartment and scanning time. The root mean square deviation of the data from the resulting best fit straight line was determined and used as a measure of the scanner linearity and the goodness of the experiment.

Corrections were made to both the uniform phantom and the linearity phantom data for positron abundance for the variety of isotopes for both the well counter and PET camera data by dividing the counts by the positron abundance, so that the results were on an actual activity basis. This correction was not necessary for the dose calibrator since automatic settings were made to correct for the effect.

The slope of the resulting linearity curve provided a value of PET camera sensitivity which was independent of the dose calibrator and the well counter, since corrections were made for well counter linearity with count rate and the PET camera background count rate was small. Sensitivities for other rings of the tomograph were determined using the relative plane sensitivities obtained from the EPS and ES studies of the longer uniformity phantom.

High count rate performance. On a monthly basis, count rate capability was verified and a check was made for the failure of various components of the system at high count rates. Deadtime loss correction was performed at reconstruction time by multiplying the observed count rates by a factor based upon the observed count rate and the experimentally determined equivalent deadtime per coincidence event (*1*). A 17.8-cm diameter, 10-cm-long uniform phantom was filled with 2600–7400 MBq (70–200 μCi) of ^{15}O, resulting in count rates in excess of 50–70 kcps/plane. It should be noted that this starting amount of activity far exceeds the useful range of linearity for the system, which is 0 to 222 kBq cm^{-3} (0 to 6 μCi cm^{-3}) (*1*). Beginning with an extreme activity, however, ensured that the useful range was completely tested, and that the various components of the system were stressed to their fullest extent.

The high activity phantom was sequentially scanned in non-wobbled mode for 12.5 half-lives (32 frames at 15 sec, 24 frames at 30 sec, 5 frames at 1 min). Images were visually checked for obvious artifacts or nonuniformities. Total counts for each plane were automatically read from the reconstructed image header and plotted. When peak count rates for any plane drifted significantly below specifications, maintenance work was performed to restore the machine to its original performance level.

Hot spot resolution phantom. Overall image quality was qualitatively checked each month by imaging a hot spot resolution phantom (*5*) filled with ^{18}F. Attenuation, uniformity, deadtime, and randoms corrections were applied to the data. The resulting reconstructed images were examined for visibility and uniformity of the individual hot spots.

Statistical Analysis

Multiple analysis of variance of the EPS data was performed using a standard software package SPSS (Statistical Package for the Social Sciences (SPSS), SPSS Inc., Chicago, IL). First, scatter plots were examined. A search was made to see whether the data could be readily separated into definite periods and whether there were any abrupt changes in behavior or gradual trends. Significant outliers in sensitivity data, which could influence the data analysis unfairly by producing apparent drifts, were investigated. These outliers were removed for the purposes of a regression analysis which was then performed on the data. Logarithms of the data were used for analysis in order to improve symmetry and assist in exploratory data analysis (*6*). If the correlation coefficient, p, was close to 1.0, then a trend was suspected. The Durbin-Watson statistic, a parameter used to determine whether or not data are autocorrelated (*7*), was examined after trends were removed by the regression. No autocorrelations were believed present if this statistic was close to 2.0.

Stem and leaf diagrams are histogram-like displays of data in which leading digits are employed as bins for the trailing digits (*8*). These hybrids between diagrams and tables were employed to search for outliers and bimodality of the distribution. P-p plots, plots of the observed residuals against the residuals expected from a normal distribution (*9*), were made and examined for linearity. Nonlinearity of p-p plots were interpreted as being diagnostic of deviations from Gaussian distributions. The magnitudes and significance of changes and variations were examined.

The results of the daily PET sensitivity experiments could be normalized either to the dose calibrator readings of activity or to the counts obtained using the well counter. Both the well counter- and dose calibrator-normalized sensitivities and their correlations were evaluated using multiple analysis of variance. After adjusting for periods of scanner malfunction, cubic splines were fit to both the well counter- and dose calibrator-normalized sensitivities. Correlations of the well counter- and dose calibrator-normalized sensitivities, fits, and residuals were evaluated.

RESULTS

Empty Port Scan Data

The EPS data are essentially obtained using the same, long-lived radiation source, and are thus free from variations in the sensitivity of ancillary equipment and in the experimental procedure. The initial scatter plots for the EPS data summed for each plane revealed that several distinct time periods existed for which different sensitivity values were best to use. This is illustrated in Figure 1 for one of the straight-across planes. The different time periods included an "early" time period, a time period for which there was a bad low voltage power supply, and a "late" time period after repair of the low voltage power supply problem. Another period of altered performance, during which the software used to collect the transmission rod source data performed masking incorrectly, was apparent with detailed regression analysis.

Arithmetic means and standard deviations of the EPS data, obtained from the logarithmically-transformed data, are included in Table 1 for all planes. As shown in this table, the use of rod source masking does not explain the behavior during the period of poor equipment performance. All planes roughly tracked the same trends during the three distinct time periods.

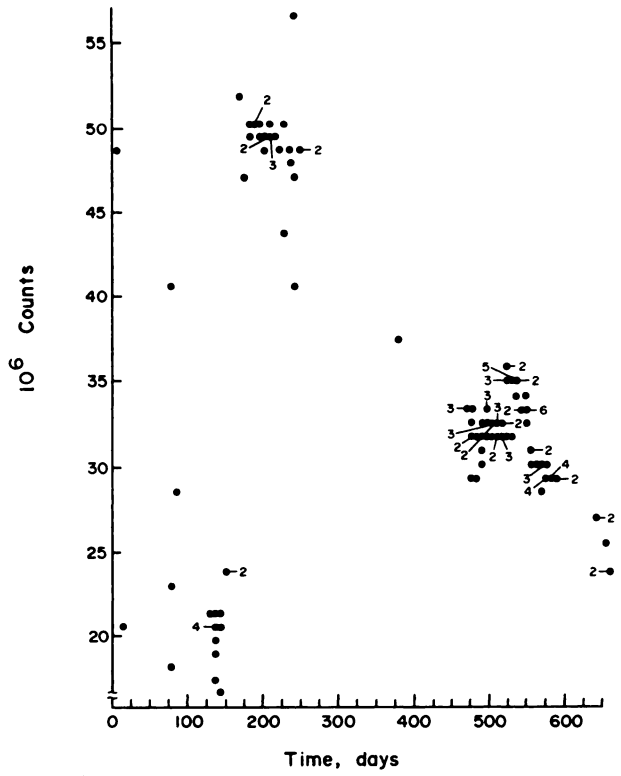

FIGURE 1
Sums of decay-corrected detector coincidences obtained for a straight across plane during empty port scans (EPS) over a time period of ~22 mo. Numbers indicate several overlapping data points with similar values.

Outliers were removed from the data and regressions were performed on each plane for sensitivity as a function of time for each period of different camera performance. The scatter plot for the data from the later time period for the straight across plane of Figure 1 is included as Figure 2A. Figure 2B shows the residuals resulting from the fit to the trend for that data, which was ln (counts) = (20.33 ± 0.04) + (−4.58 ± 0.01 × 10^{-3}) * t (days), with $p < 0.0001$. The corresponding p-p plot, indicating a normal distribution after removal of the trend, appears as Figure 2C. By using distinct time periods and characterizing trends within the time period, as illustrated here, it was felt that improved absolute and relative calibrations data were obtained for each plane.

Emission Scan Data

A stem and leaf diagram of the PET sensitivity values, obtained using the emission scan (ES) for one plane of data, is included as Figure 3. This useful diagram was quick and simple to construct. The ES data represented begin at a time corresponding to day 584 of the EPS data in Figure 1. Bimodality of the distribution indicating a period of poor performance, related the failure of voltage supply failure, is clearly apparent. The failure affected only the first three rings of the PET camera. Outliers are also readily distinguished in the stem and leaf diagram.

Table 2 shows the mean and standard deviations for the ES sensitivity data obtained during the time period of the stem and leaf diagram. Extreme outliers were excluded from this analysis. These data roughly track the EPS data but show a larger standard deviation because of the additional experimental variables and data manipulations involved.

Phantom Repositioning Accuracy

The standard deviation of the distance from the center of the field of view to an ellipse encompassing images of transmission scans of the uniform phantom on 77 different days was 2.7 mm without the captive rail. With the laser system and modified couch, no difference in location of ellipse encompassing images of

TABLE 1
Decay-Corrected Million Counts Obtained for Individual Imaging Planes Using EPS Data

	A*	B†	B1‡	B2§	C¶
No. points	25	46	22	24	92
Plane 1	39.4 ± 2.0	20.0 ± 0.8	19.7 ± 0.8	20.4 ± 0.6	14.5 ± 2.7
Plane 1/2	33.3 ± 3.1	15.7 ± 0.8	14.9 ± 0.5	16.5 ± 0.5	17.7 ± 2.9
Plane 2	35.3 ± 0.2	19.6 ± 1.0	18.8 ± 0.4	20.6 ± 0.6	22.5 ± 3.9
Plane 2/3	28.6 ± 8.1	15.1 ± 1.4	14.1 ± 0.9	15.9 ± 1.0	16.9 ± 3.1
Plane 3	44.9 ± 2.3	20.2 ± 1.2	19.4 ± 0.8	21.0 ± 0.9	23.2 ± 4.3
Plane 3/4	25.6 ± 23.5	16.5 ± 1.6	15.2 ± 0.5	17.7 ± 1.1	17.9 ± 2.5
Plane 4	30.0 ± 128	28.6 ± 1.8	27.2 ± 0.8	30.1 ± 0.9	26.4 ± 3.4
Plane 4/5	30.0 ± 13	22.5 ± 1.6	21.0 ± 0.6	23.9 ± 1.0	20.8 ± 2.7
Plane 5	47.2 ± 2.9	30.1 ± 1.5	29.2 ± 0.9	31.3 ± 1.0	28.1 ± 3.6

* Early period.
† Bad period, all data.
‡ Bad period, no masking.
§ Bad period, masking.
¶ Late period.
Data are divided into an early period, a bad period during which time a voltage supply had failed, and a late period (these time periods do not overlap). The means and standard deviations were obtained for logarithmically transformed data.

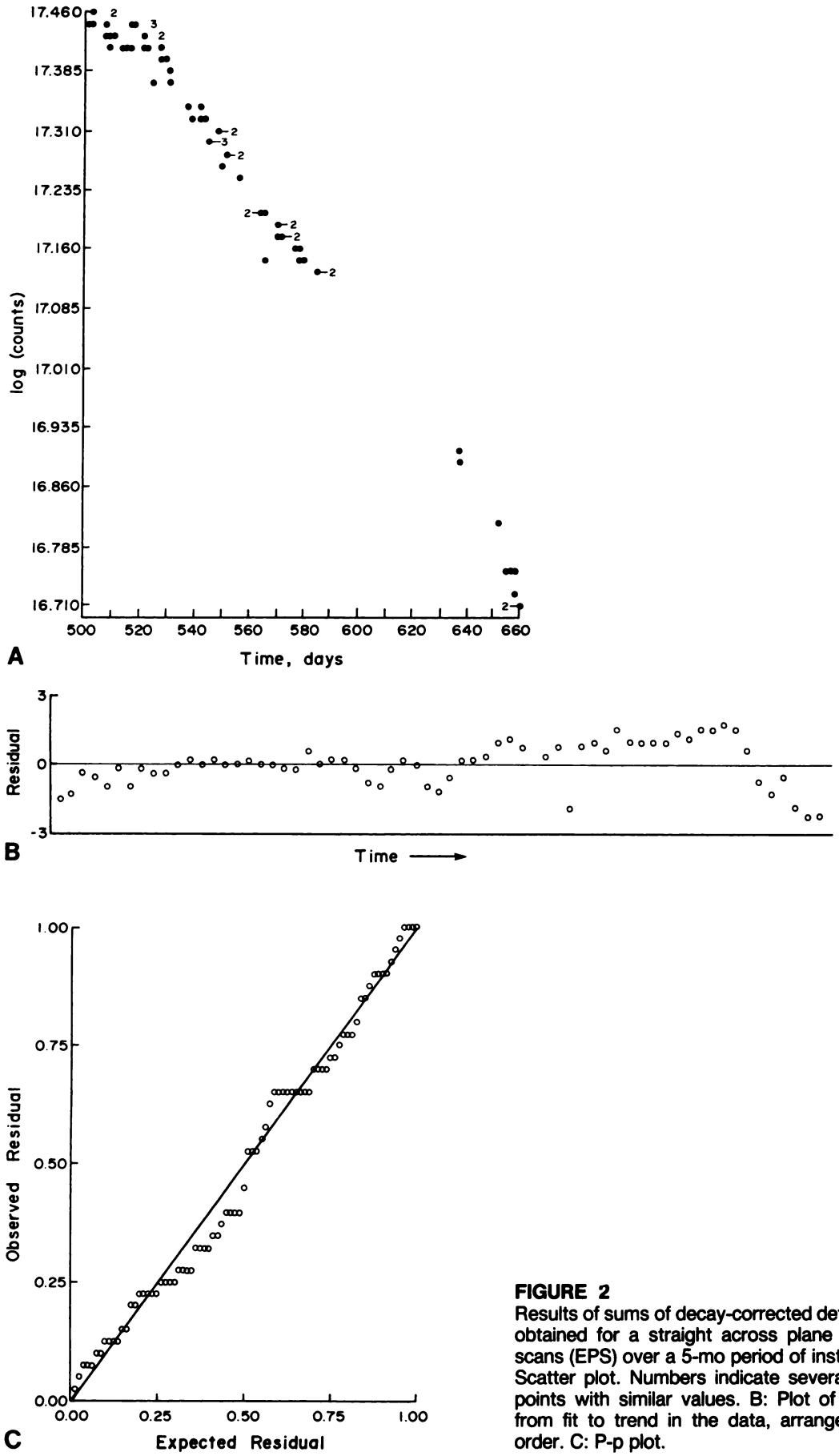

FIGURE 2
Results of sums of decay-corrected detector coincidences obtained for a straight across plane during empty port scans (EPS) over a 5-mo period of instrument stability. A: Scatter plot. Numbers indicate several overlapping data points with similar values. B: Plot of residuals resulting from fit to trend in the data, arranged in chronological order. C: P-p plot.

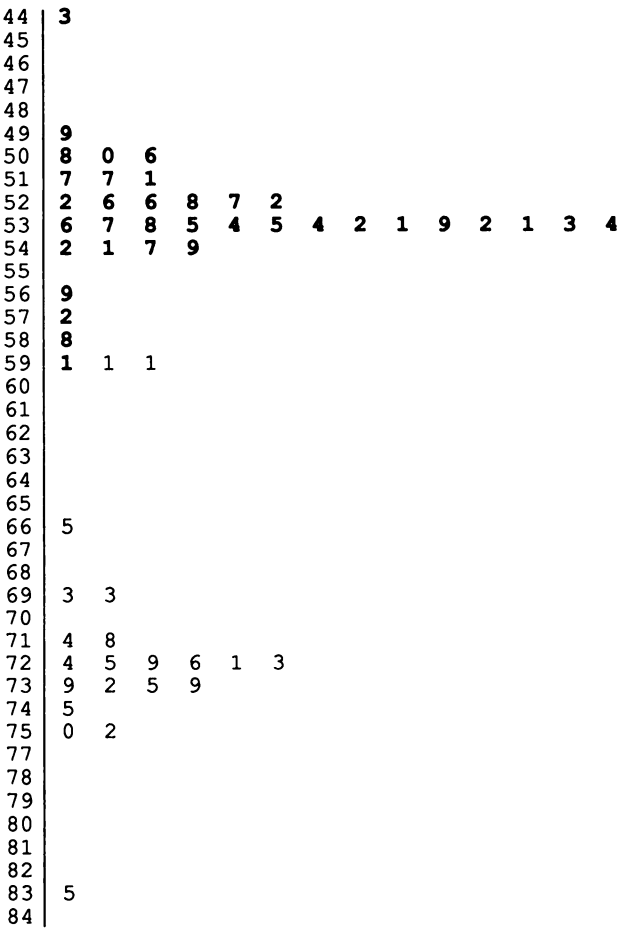

FIGURE 3
Stem and leaf diagram of PET camera sensitivity for a straight across plane obtained using emission scans (ES) over a 3-mo period. Numbers to the left of the vertical bar represent leading digits of the sensitivity value expressed as kcps μCi^{-1} cm^{-3}. Numbers to the right of the vertical bar represent the least significant digits. The top number thus corresponds to a value of 44.3 kcps μCi^{-1} cm^{-3}, while the bottom data point represents 83.5 kcps μCi^{-1} cm^{-3}. Bold numerals correspond to a time period of decreased instrument sensitivity during the middle of the testing period.

the transmission scans of the uniform phantom was obtained for 19 days. Thus the repositioning of the phantom was believed to be to within <1 mm in the transverse dimension. The effects of position on sensitivity were determined to be small for reasonable motions within the scanner port, 0.8 ± 0.8% of the sensitivity value for a 1-cm displacement, with slightly greater changes being observed for the cross-planes. However, accurate positioning is especially important when scans made on the same patient on different days are to be correlated and for cases in which movement of phantoms or patients occurs between the collection of the transmission data and the emission data. Because of the repositioning accuracy of the modified couch, the same attenuation correction factors could have been used for daily PET QA on days not markedly separated in time, resulting in a time savings.

TABLE 2
PET Sensitivity Obtained from Daily ES of a Long, Uniform Phantom, Expressed as kcps μCi^{-1} cm^{-3}

Time period	A	B	A + B
No. points	21	32	52
Plane	Sensitivity (kcps μCi^{-1} cm^{-3})		
1	71.6 ± 5.2	53.2 ± 2.5	60.4 ± 9.4
1/2	89.7 ± 5.8	66.1 ± 2.7	64.7 ± 10.2
2	77.7 ± 4.6	56.5 ± 2.3	59.8 ± 10.8
2/3	98.2 ± 7.5	68.6 ± 3.9	75.3 ± 11.6
3	73.2 ± 4.5	51.4 ± 2.9	79.9 ± 14.7
3/4	84.3 ± 5.1	64.7 ± 3.2	72.4 ± 9.5
4	65.2 ± 2.8	69.8 ± 2.3	68.2 ± 3.5
4/5	80.6 ± 4.0	85.9 ± 2.7	84.1 ± 4.4
5	68.0 ± 3.6	71.0 ± 2.0	69.8 ± 3.9

Time period A includes days 584–640 and 704–718, whereas time period B corresponds to days 641–703, a time of voltage supply failure which affected the first three scanner rings.

Well Counter Versus Dose Calibrator Normalization

Monitoring of the well counter 26 times over a 70-day period and the dose calibrator monthly over a 1-yr period using long-lived radioisotope sources did not reveal any obvious drifts in the equipment response. Furthermore, initial examination of the daily well counter- and dose calibrator-normalized PET camera sensitivities obtained using short-lived positron-emitting isotopes did not reveal any significant correlations. However, when daily variations were removed using spline fits, the sensitivities did correlate very significantly positively. Hence, once the day-to-day variations in the splines were removed by fitting, similar long-range drifts were indicated in both the well counter- and dose calibrator-normalized sensitivities. Since the well counter and dose calibrator are essentially independent instruments, these drifts were presumably due to drifts in the actual PET scanner sensitivity. A better idea of the nature of the PET scanner sensitivity drifts can be made, however, by analyzing the EPS data, as discussed above.

The residuals of the well counter- and dose calibrator-normalized sensitivities, which were adjusted to the drifts fit by the splines, were only very slightly negatively correlated. This negative correlation could indicate some dependence upon the exact amount of activity used for the experiments, or an effect of room temperature or power supplied to the room which could have affected these instruments in opposite ways.

The standard deviation of the residuals of cubic spline fits of PET sensitivity as a function of time was twice as large for well counter-normalized data, 1.0%, than for dose calibrator-normalized data, 0.5%. The use of the well counter for PET sensitivity normalization thus introduces a greater uncertainty in the measurements than the dose calibrator.

Sensitivity Computations

Data from the linearity phantom were utilized to compute the sensitivity on a per pixel basis. The effects of attenuation, deadtime, randoms and inhomogeneity corrections and the reconstruction on the image were included in the linearity data. Effects of changing the Hanning ramp reconstruction filter cutoff frequency from 0.8 to 1.4 was <0.6% for these measurements, indicating the general insensitivity of the calibrations on filter choice. The stability of the results on ROI placement was determined to be excellent by comparing values obtained using several 12 cm^2 ROIs with those obtained using a single 615 cm^2 ROI in 24 images of the uniformity phantom. The standard deviations of the values were 7–13% for both ROI types selected. The overall average sensitivities determined using the larger ROIs were only 1% less than those obtained with the smaller ROIs.

Because the daily ES data of the uniform phantom resulted from an activity distribution similar to that of many patient studies (unlike the EPS), these proved useful for extrapolating the relative sensitivities for each plane. The fitted EPS data provided the best information about trends and drifts, and were therefore used to extrapolate sensitivity values for each day or period of operation.

Other Phantom Studies

The high count rate studies proved useful in discovering and rapidly diagnosing component failures appearing at the high count rates encountered for some studies. No particular information about camera performance not obtained by other means was revealed by the use of the hot spot resolution phantom.

DISCUSSION AND CONCLUSIONS

The daily PET QA experiments required <1 hr of machine time, and could be substantially shortened for more sensitive, newer generation systems. The protocols tested PET scanner under its various conditions of use and provided both absolute and relative calibration data. The daily emission and transmission scans of a uniform, long phantom provided the operator with immediate feedback on instrument problems which may have been developing. The long-lived $^{68}Ge/^{68}Ga$ transmission rod source, utilized for collecting the empty port scans (EPS), was best for detecting and characterizing slow, long-term drifts in PET sensitivity.

Daily tuning of the energy windows of the system was essential for stabilizing performance in the presence of environmental variations affecting PMT gains. Equipment was left on at all times for added stability. It should be noted that the PC 4600, an older generation PET system, has only one crystal per PMT, while more modern systems have multiple crystals coupled to each PMT. From this viewpoint, the problem of system tuning and QA as a whole could be even more important for newer systems. Improvements over the past few years in crystal and PMT quality should moderate this situation somewhat.

Couch modifications may result in the elimination of a standard deviation in positioning accuracy of up to 2.7 mm, depending upon the couch type. Repeatability in repositioning allows one to utilize the same attenuation coefficients each day for the daily PET QA, decreases setup time and improves quantitation for repeated studies of the same patient.

Dose calibrator normalization of PET sensitivity data resulted in a standard deviation in PET sensitivity one half that obtained for well counter-normalized data. However, it should be noted that it is the relative well counter-to-PET camera sensitivity that is of interest for absolutely calibrating PET patient studies. The EPS data are essentially free from the effects of ancillary data, and are thus preferred for monitoring the PET camera for drifts, but do not provide adequate absolute calibration information because of the geometry of the source. The slope of the PET camera linearity curve provides a good alternative for absolute machine calibration.

Results of the linearity phantom sensitivities were in good agreement with the daily PET QA results obtained using the longer, uniform phantom. The linearity phantom also provided confirmation of the calibrations for a different source configuration and for a situation in which all image corrections were applied. One disadvantage of the particular linearity phantom used as that it did not cover all planes of the scanner simultaneously.

High count rate scans were invaluable in verifying PET scanner performance under the conditions encountered for PET studies involving large bolusses of short-lived activity or hot spots. The occasional scanning of the hot spot resolution phantom could be useful in monitoring machine performance, since it provides a more complex image in which overall spatial resolution and resolution uniformity could be quickly noted. However, during the time period reported here, the hot spot resolution phantom revealed no information not obtained by the other studies. In the future, software should be developed to provide a quantitative measure of image uniformity, such as pixel-to-pixel standard deviation, from the low and high count rate scans of the uniformity phantom.

Corrections for scatter, attenuation, deadtime, randoms and detector inhomogeneity all affect machine sensitivity. However, if the calibration experiments are designed to closely resemble the geometry and count rates encountered during instrument use and if the corrections are properly performed, adequate system calibrations may be achieved.

The use of the EPS data provides information about

camera performance which was independent of well counter and dose calibrator behavior, since the same $^{68}Ga/^{68}Ge$ transmission rod source was used for obtaining the data each day. Such data, however, do not truly test the system in the manner in which it is used: The EPS scans are collected using a source moved around the edge of the port, whereas typical PET studies involve positron emitter distributed fairly uniformly in the 20-cm-diameter field of view centered in the scanner port. In analyzing EPS data over an extended period of time, proper correction must be made for decay of the $^{68}Ga/^{68}Ge$ source, and it should therefore be relatively free of short and long-lived radioisotopic impurities. Other background radioisotopes could also influence the study of scanner drift determined in this manner. Collection and analysis of EPS data proved invaluable in deciding when significant changes in sensitivity had occurred in any given plane. Ultimately, the behavior of each individual detector could be monitored over time using the EPS data, with software automatically signalling the user when excessive drift or aberrant behavior was occurring.

ACKNOWLEDGMENTS

This work was supported in part by HEW Public Health Services award number NS 15665 and National Science Foundation award number ECE 8451542. Special thanks are extended to John Conti, Paula Carmichael, Howard Thaler, and Robert Rucker for their assistance with this work.

REFERENCES

1. Kearfott KJ, Carroll LR. Evaluation of the performance characteristics of the PC 4600 positron emission tomograph. *J Comput Asst Tomogr* 1984; 8:502–513.
2. Conti J, Deck MDF, Rottenberg DA. Technical note. An inexpensive video patient repositioning system for use with transmission and emission computed tomographs. *J Comput Asst Tomogr* 1982; 6:417–421.
3. Kearfott KJ, Rottenberg DA, Knowles RJR. Technical note. A new headholder for PET, CT, and NMR imaging. *J Comput Asst Tomogr* 1984; 8:1217–1220.
4. Eichling JO, Higgins CS, Ter-Pogossian MM. Determination of radionuclide concentrations with positron CT scanning (PETT): Concise communication. *J Nucl Med* 1977; 18:845–847.
5. Derenzo SE, Budinger TF, Cahom JL, Huesman RH, Jackson HG. High resolution computed tomography of positron emitters. *IEEE Trans Nucl Sci* 1977; NS-24:544–558.
6. Tukey JW. Easy re-expression. In: *Exploratory data analysis.* Reading: Addison-Wesley Publishing Company, 1977: 57–96.
7. Wonnacott TH, Wonnacott RJ. Time series analysis. In: *Introductory statistics for business and economics.* Santa Barbara: John Wiley and Sons, 1977:603–636.
8. Chambers JM, Cleveland WS, Kleiner B, Tukey PA. Stem and leaf diagrams. In: *Graphical methods for data analysis.* Boston: Duxbury Press, 1983:26–29.
9. Chambers JM, Cleveland WS, Kleiner B, Tukey PA. Properties of the theoretical quantile-quantile plot. In: *Graphical methods for data analysis.* Boston: Duxbury Press, 1983:197–203.